Magnetic moments of ^{17}N and ^{17}B

H. Ueno,* K. Asahi, H. Izumi, K. Nagata,† H. Ogawa, A. Yoshimi, H. Sato, M. Adachi, Y. Hori,‡ and K. Mochinaga
Department of Applied Physics, Tokyo Institute of Technology, Oh-okayama 2-12-1, Meguro-ku, Tokyo 152, Japan

H. Okuno,§ N. Aoi, and M. Ishihara‖
Department of Physics, University of Tokyo, Hongo 7-3-1, Bunkyo-ku, Tokyo 113, Japan

A. Yoshida, G. Liu,¶ T. Kubo, and N. Fukunishi
Institute of Physical and Chemical Research (RIKEN), Hirosawa 2-1, Wako-shi, Saitama 351-01, Japan

T. Shimoda, H. Miyatake, M. Sasaki, T. Shirakura, and N. Takahashi
Department of Physics, Osaka University, Machikaneyama 1-16, Toyonaka, Osaka 560, Japan

S. Mitsuoka**
Department of Physics, Kyushu University, Hakozaki 6-10-1, Higashi-ku, Fukuoka 812, Japan

W.-D. Schmidt-Ott
Zweites Physikalisches Institut, Der Universität Göttingen, Bunsenstrasse 7-9, D-3400 Göttingen, Germany
(Received 28 November 1995)

The magnetic moments of ^{17}N and ^{17}B were measured by using spin-polarized radioactive nuclear beams which were obtained from the projectile fragmentation reaction. The observed magnetic moment of ^{17}N, $|\mu(^{17}\mathrm{N})|=(0.352\pm0.002)\mu_N$, where μ_N is the nuclear magneton, falls outside the Schmidt lines. By virtue of a simplifying feature of nuclear structure inherent in a $p_{1/2}$ valence nucleus, the deviation from the Schmidt value is attributed on firm ground to admixing of the configurations in which two neutrons in the sd shell are coupled to $J^\pi=2^+$. This interpretation is confirmed in standard shell-model calculations. The calculations reproduce fairly well the experimentally inferred amount of 2^+ admixture, as well as the experimental magnetic moment itself. The magnetic moment for ^{17}B was determined as $|\mu(^{17}\mathrm{B})|=(2.545\pm0.020)\mu_N$. The result is substantially smaller than the $\pi p_{1/2}$ single-particle value, and the shell-model calculations indicate that the quenching of μ largely stems from $J^\pi=2^+$ configurations of the sd neutrons. The observed amount of quenching, however, is larger than the shell-model predictions, suggesting an enhanced contribution of the 2^+ neutron configurations. This result is explained if the pairing energy for neutrons in the sd shell of a neutron-rich nucleus is assumed to diminish by about 30%. We also find that the use of the reduced pairing energy improves agreements in the magnetic moment and low-lying energy levels of ^{17}N as well. [S0556-2813(96)05005-4]

PACS number(s): 21.10.Ky, 21.60.Cs, 24.70.+s, 27.20.+n

I. INTRODUCTION

The knowledge of nuclear structure has been traditionally based on data obtained in the region of nuclei close to the stability line. Recently, a new experimental method [1] to produce unstable nuclei has been developed. It uses the projectile fragmentation reaction induced by an intense beam of heavy ions accelerated to energies of the order of 100 MeV/nucleon or higher and relies on a scheme of the in-flight isotope separation in terms of the magnetic rigidity and momentum loss in a degrader. It has enabled studies of light neutron-rich and proton-rich nuclei, and measurements of properties such as masses, radii, lifetimes, and decay modes have been performed. Several intriguing features have been revealed in this class of nuclei, and interest in their nuclear structure has been renewed. As a further step, experimental studies which probe microscopic aspects such as the configurations of nucleons are most desirable.

We have been developing a method to obtain spin-polarized unstable nuclei by using the projectile fragmentation reaction, aiming at the measurement of nuclear moments. By its application we previously measured the magnetic moments [2] and the electric quadrupole moments [3] for ^{14}B and ^{15}B. In the present work, we report on the measurement of the magnetic moment for ^{17}N ($I^\pi=1/2^-$, $T_{1/2}=4.173$ s, $Q_\beta=8.680$ MeV) and ^{17}B ($I^\pi=3/2^-$, $T_{1/2}=5.08$ ms, $Q_\beta=22.99$ MeV [4]). As discussed later, the configuration of excess neutrons in ^{17}N can be determined

*Present address: Laboratory of Nuclear Studies, Osaka University, Machikaneyama 1-1, Toyonaka, Osaka 560, Japan.
†Present address: Broadband Network Systems Laboratory, Nippon Telegraph and Telephone Corporation, Midori-cho 3-9-11, Musashino-shi, Tokyo 180, Japan.
‡Present address: Toshiba Corporation, Shibaura 1-1-1, Minato-ku, Tokyo 105, Japan.
§Present address: Institute of Physical and Chemical Research (RIKEN), Hirosawa 2-1, Wakoshi, Saitama 351-01, Japan.
‖Also at Institute of Physical and Chemical Research (RIKEN), Hirosawa 2-1, Wako-shi, Saitama 351-01, Japan.
¶Present address: Institute of Modern Physics, Chinese Academy of Science, 253 Nanchang Road, Lanzhou, Gansu Province 730000, People's Republic of China.
**Present address: Research Center for Nuclear Physics, Osaka University, Mihogaoka 10-1, Ibaraki-shi, Osaka 567, Japan.

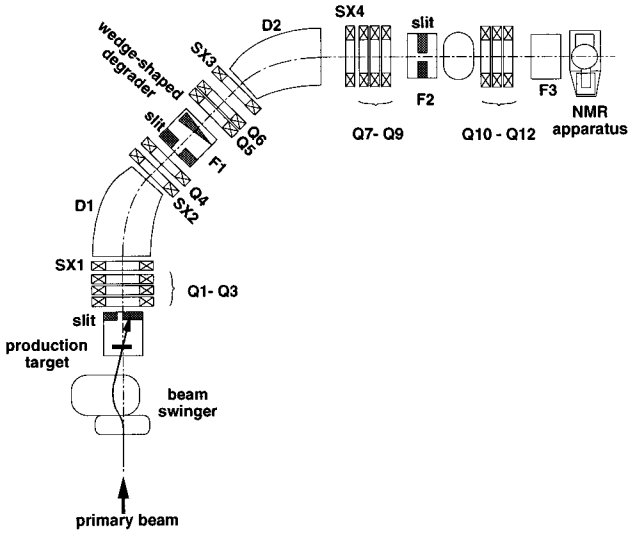

FIG. 1. Schematic drawing of the setup for the production, separation, and implantation of spin-polarized fragments using RIPS. $D1$ and $D2$ designate the dipole magnets, $Q1-Q12$ the quadrupole lenses, SX1–SX4 sextupole lenses, and $F1-F3$ the focuses. The center value for the fragment emission angles up to 15° can be chosen by using the beam swinger which consists of a pair of dipole magnets. The NMR apparatus for the measurement of the magnetic moments is installed at $F3$.

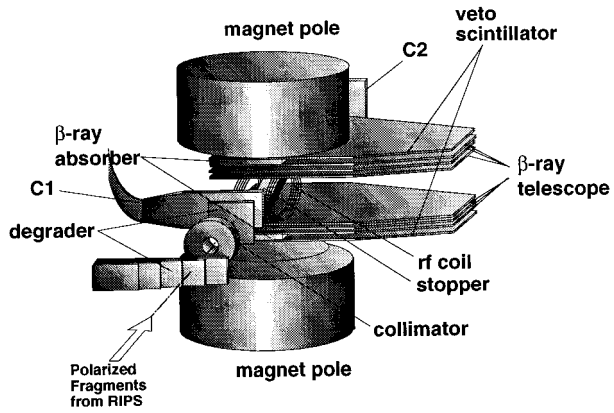

FIG. 2. Experimental arrangement for the nuclear magnetic resonance measurement. A beam of polarized fragments from RIPS is introduced as indicated by the arrow. $C1$ and $C2$ are plastic scintillators used for the tuning and monitoring of the fragment implantation into the stopper. $C1$ is used also as the veto scintillator in order to reject the background β rays emitted from the degrader. A static magnetic field B_0 is applied with the poles of an iron-core electromagnet. An oscillating magnetic field B_1 is applied by using the rf coil wound around the stopper. The β rays emitted from the fragments implanted in the stopper are counted by the β-ray telescopes above and below the stopper.

quite reliably from the experimental magnetic moment, owing to the unique feature of a nucleus having a $p_{1/2}$ valence nucleon. The data thus delineate how the excess neutrons are coupled, which is prerequisite to understand the characteristic features of neutron-rich nuclei. The nucleus ^{17}B, having more than twice the number of neutrons than of protons and a two-neutron separation energy as small as 1.39 MeV [5], may represent a typical example of neutron-rich nuclei. Recent data suggested that ^{17}B is associated with a neutron halo [6].

II. EXPERIMENTAL PROCEDURE

A. Production and implantation of polarized fragments

A beam of ^{17}N fragments was obtained from the fragmentation of ^{18}O projectiles at an average energy of 64.7 MeV/nucleon on a ^{93}Nb target of 0.429 g/cm^2 thickness. In order to have the ^{17}N fragments spin polarized [7,8], the emission angle and the outgoing momentum were selected for the fragments. Thus the ^{17}N fragments emitted at $\theta_L=2.5\pm1.0°$ were transmitted to the fragment separator RIPS [9], where the momentum region of $p=5.82$–5.88 GeV/c was selected. A schematic view of RIPS is shown in Fig. 1. To attain the setting of $\theta_L\neq0$, which was essential for obtaining the nonvanishing spin polarization, a beam swinger installed upstream of the target was used. The isotope separation was provided through the combined analyses of the magnetic rigidity and momentum loss. An achromatic aluminum degrader of a wedge shape with a median thickness of 426 mg/cm^2 and a slope angle of 2.21 mrad was inserted in the path of the fragment beam at the momentum-dispersive focal plane $F1$. The degrader produced a momentum shift proportional to $A^{2.5}/Z^{1.5}$, which in turn was converted by the second dipole magnet into a physical separation of the isotopes at the focus $F2$. Here A and Z denote the mass and charge numbers of the fragment. The term ''achromatic'' means that the slope of the wedge thickness is tuned such as to attain a constant relative momentum loss $\delta p/p$ for the actual fragments, so that the achromaticity for the fragments is restored by the second dipole, which is almost symmetrical to the first one. The fragments were identified by means of the measurement of the energy loss in a 500-μm-thick Si detector located at $F2$ and the time of flight (TOF) between an anode signal of a position-sensitive parallel plate avalanche counter (PPAC) [9] at $F2$ and a signal synchronous with the primary beam, derived from the accelerator rf system.

The ^{17}N fragments were transported from $F2$ via a quadrupole triplet to the setup schematically shown in Fig. 2. They were implanted into a graphite stopper placed at its center. The material for the stopper was chosen to provide a spin-relaxation time T_1 which is longer than the nuclear lifetime. A static magnetic field $B_0=247.5$ mT was applied to the stopper in order to preserve ^{17}N spin polarization.

Similar procedures were taken for the measurement of the ^{17}B magnetic moment. For the production of ^{17}B fragments, a beam of ^{22}Ne at an average energy of 94.4 MeV/nucleon and a ^{93}Nb target of 1.07 g/cm^2 thickness were used. An emission angle of $\theta_L=1.5\pm1.0°$ and a fragment momentum window of $p=7.13$–7.57 GeV/c were selected. An achromatic degrader with a median thickness of 1638 mg/cm^2 and a slope angle of 8.67 mrad was chosen for the isotope separation of ^{17}B. The production cross section for ^{17}B was estimated to be as small as $\sim$100 nb based on the systematics and the use of the simulation code of Ref. [10]. In order to overcome the difficulty due to the small production yield, a relatively thick target and wide momentum region were cho-

sen. In addition, β-ray telescopes with solid angles 2.5 times larger (50% of 4π in total) than those used in the ^{17}N experiment were developed. The rejection of background events due to cosmic rays was implemented by a veto scintillator, which, in conjunction with a β-ray absorber, was installed behind each β telescope. After such improvements in the apparatus, a count rate of β rays as large as 3–4 counts/s was obtained. A stopper consisted of a stack of six Pt foils, each 140 μm thick. The relaxation time T_1 for B isotopes in Pt at room temperature is known to be much longer ($\gtrsim$300 ms for ^{17}B [11]) than the ^{17}B lifetime of 7.26 ms. A static magnetic field of B_0=100.0 mT was applied to the stopper.

B. Detection of the nuclear magnetic resonance

The magnetic moments of the fragments were measured by means of nuclear magnetic resonance (NMR). After the polarized fragments were implanted in the stopper, a radio-frequency oscillating field B_1 was applied in the direction perpendicular to B_0 by exciting a rf coil mounted around the stopper as shown in Fig. 2. In order to detect the NMR, β rays emitted from the fragments in the stopper were detected by using plastic scintillator telescopes located above and below the stopper.

In the present experiment, the adiabatic fast passage (AFP) method of the NMR technique [12] was applied. In this method, the frequency for B_1 is swept over a region of width $\delta\nu$. If the region includes the Larmor frequency ν_0, which is given by

$$\nu_0=\frac{\mu B_0}{hI}, \tag{1}$$

the spins of the implanted fragments are reversed through the NMR. Here I and μ denote spin and magnetic moment of the fragment nucleus, and h is Planck's constant. The reversal of the fragment spins is detected through the observation of the up/down asymmetry in the β decays of the fragments. The angular distribution $W(\theta)$ for the β rays emitted from nuclei with the spin polarization P is given by

$$W(\theta)=1+\frac{v}{c}A_\beta P\cos\theta, \tag{2}$$

where θ denotes the angle between the direction of the β emission and the axis of the nuclear polarization, v and c the velocities of the β particles and of light, and A_β the asymmetry parameter. For the sake of simplicity we take the approximation that $v/c\simeq 1$, since only a high-energy portion of the β spectrum was included in the analysis. Based on the observed [13] (calculated [14]) decay scheme, the value of A_β for the decay of ^{17}N (^{17}B) is estimated as $+0.57$ (-0.81). Then the up/down ratio R of the β-ray yields is expressed as

$$R=a\,\frac{(1+A_\beta P)}{(1-A_\beta P)}\simeq a(1+2A_\beta P), \tag{3}$$

where a is a constant factor representing asymmetries in the counter solid angles and efficiencies. When the polarization P is altered due to spin reversal, a change appears in the ratio R. Thus the resonance frequency ν_0 is derived from the observed peak or the dip in the R spectrum.

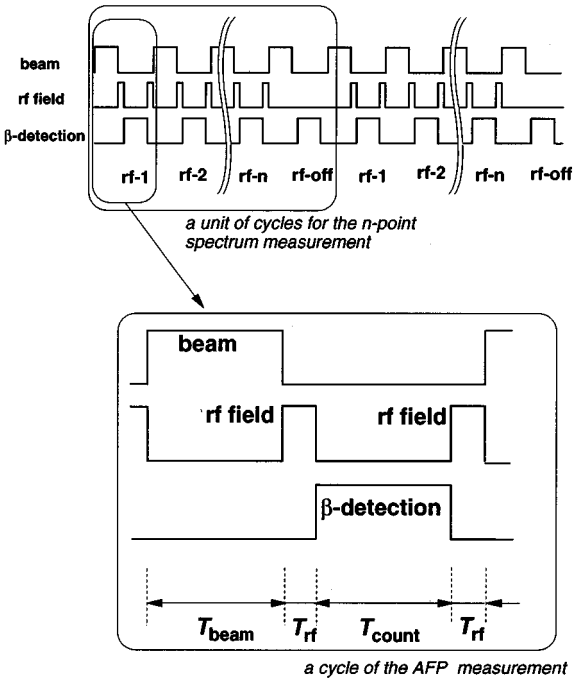

FIG. 3. Time chart for the NMR measurement. $T_{\rm beam}$, $T_{\rm rf}$, and $T_{\rm count}$ are the lengths of time for the beam bombardment, the application of the rf field, and the β-ray detection. rf-i, for $i=1,2,\ldots,n$, refer to the measurement cycles with the B_1 field frequency swept over ν_i through $\nu_i+\delta\nu$, while the cycle without B_1 application is denoted by ''rf off.''

The measurement was performed in the time sequence illustrated in Fig. 3. The beam in the ^{17}N (^{17}B) experiment was pulsed with a beam-on period of 1 s (8 ms) and a beam-off period of 11.03 s (10 ms). At the beginning of the beam-off period, the oscillating field B_1 was applied for 15 ms (1 ms) duration, with its frequency swept from ν_1 to $\nu_1+\delta\nu$. Then the β rays were counted during the following 11 s (8 ms). In the remaining 15 ms (1 ms), the oscillating field was applied again in the same scheme in order to restore the spin direction so that the up/down ratio in the succeeding cycle might not be affected by the surviving activities. In the following $n-1$ cycles, the above procedure was repeated, with the range of the frequency sweeping from ν_i to $\nu_i+\delta\nu$ ($i=2,3,\ldots,n$), and then a cycle without the application of B_1 was performed. These $n+1$ cycles, as a unit of cycles for the n-point spectrum measurement, were repeated many times to obtain a sufficient counting statistics. The number n of the frequency points typically took a value of 3–7.

The time sequence of the measurement described above was controlled by a CAMAC module, a programmed sequence generator (PSG), which was specially designed for this purpose. The sequence was expressed as a train of steps, each of them representing the instantaneous values of the frequency and amplitude of the B_1 field, the beam on/off flag, the gate signal for the counters, and the duration time for the step. The step data were loaded into a memory of the PSG module. When a signal level at the RUN input of the PSG became high, the sequence started from the initial step. The PSG continued to run until the low level was detected at the RUN input at the end of the unit of cycles. The block diagram for the sequence control is shown in Fig. 4.

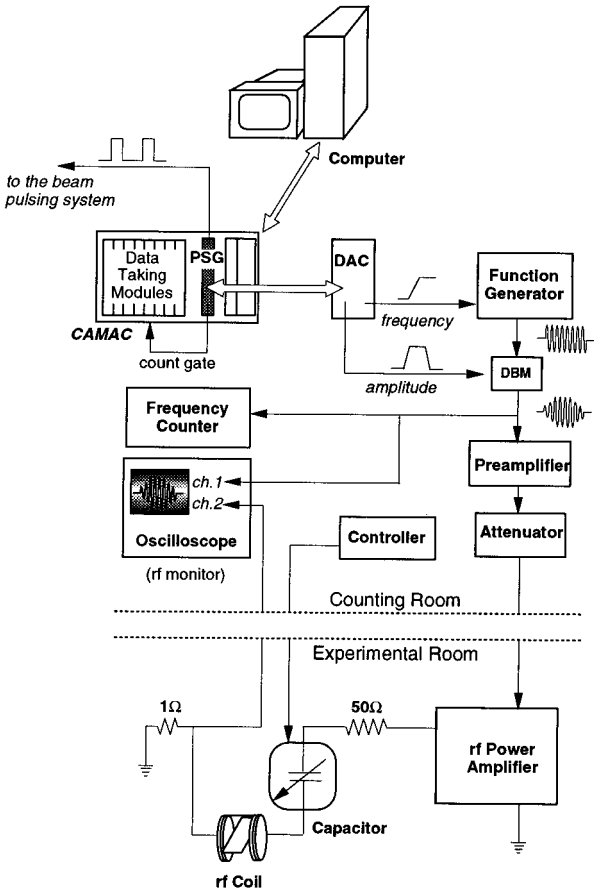

FIG. 4. Block diagram of the electronics for the control of the NMR measurement. PSG, programmed sequence generator; DAC, digital-to-analog converter; DBM, double-balanced mixer. The PSG produces a beam-blocking signal, a gate signal for the β counting, and digital data which specify the frequency and amplitude of the B_1 field, according to a list of data preloaded into the PSG memory from a computer through the CAMAC interface.

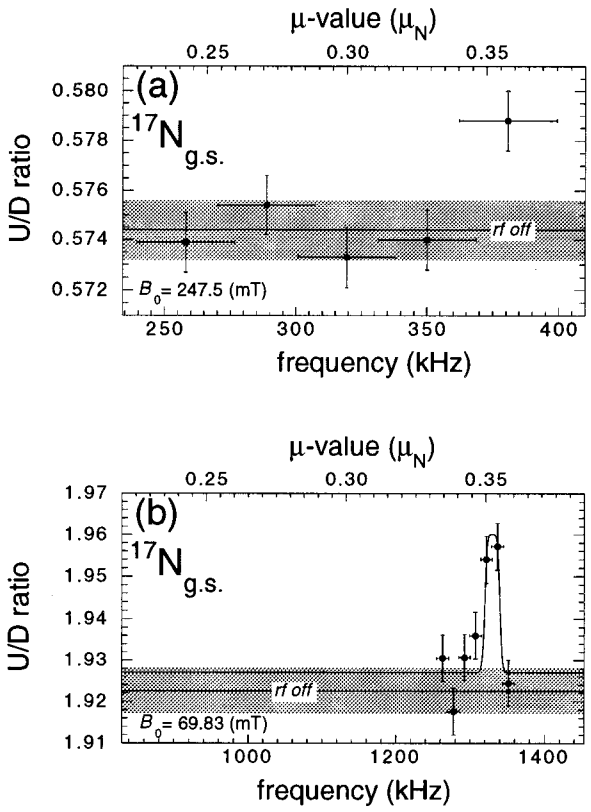

FIG. 6. NMR spectrum obtained for ^{17}N, with the bin widths (a) $\delta\nu/\nu$=9.9% and (b) $\delta\nu/\nu$=1.2%. For each experimental point the statistical error and the width of the frequency sweep are indicated by the vertical and horizontal bars, respectively. The R value without application of the rf field is indicated by the horizontal line, and its statistical error by the shadow. After the μ value was found to lie in the region (0.340–0.375)μ_N from the result (a), the measurement was made by dividing this region into seven narrow bins in (b). For the fitted curve in (b), see the text.

III. RESULTS OF THE EXPERIMENT

The time spectrum obtained for the β-ray events in the ^{17}N experiment is shown in Fig. 5. The spectrum was fitted with an exponential function with the known half-life [13] $T_{1/2}(^{17}\mathrm{N})$=4.173 s and a constant background. The resulting χ^2 value of 1.15 confirmed that the ^{17}N isotope was correctly identified in the implantation procedure. In the case of ^{17}B, the β-ray time spectrum was fitted with the same functional form, but with $T_{1/2}$ as one of the fitting parameters. The result, $T_{1/2}$=5.07±0.21 ms, was in good agreement with the reported value for ^{17}B, $T_{1/2}(^{17}\mathrm{B})$=5.08±0.05 ms [15].

In Figs. 6 and 7 the up/down ratio R observed as a function of the frequency ν of the B_1 field is plotted for ^{17}N and ^{17}B. In these plots, a deviation of R from the value obtained without application of the B_1 field (denoted as ''rf off'' in the figures) indicates the occurrence of a spin alteration by the AFP method, as discussed in Sec. II B. Note that ^{17}N and ^{17}B have opposite observed deviations. This is due to the fact that the signs of the asymmetry parameters A_β are different, while the polarizations of these two fragments have the same

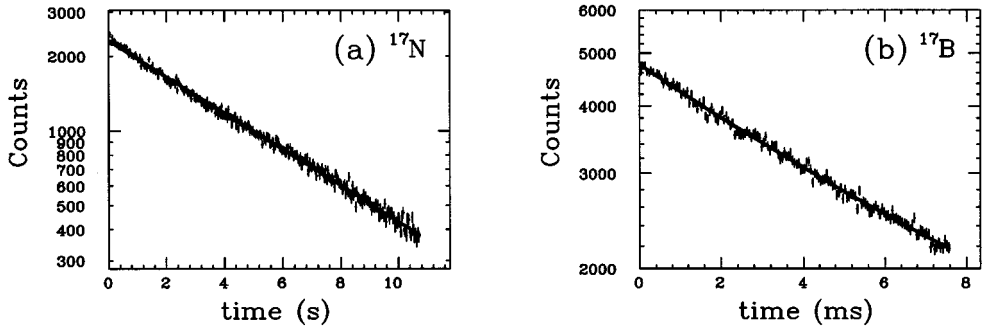

FIG. 5. Time spectra obtained for the β-ray events in the ^{17}N and ^{17}B experiments. The curves show the result of a least-χ^2 fitting of an exponential plus a constant background to the data.

sign. The degrees of polarization obtained for ^{17}N and ^{17}B were both around -1%.

To obtain the peak frequency ν_0, the observed R spectrum for ^{17}N was fitted with a function $R(\nu)$ given as

$$R(\nu)=C_1\exp\left[-C_2\exp\left(\frac{\nu-\nu_0}{\sigma}\right)^2\right]+C_3. \tag{4}$$

Here C_1, C_2, C_3, and ν_0 are the free parameters for the fitting. The functional form (4) was chosen so as to reproduce the result of a computer simulation of the AFP spin reversal process. In the simulation, the motion of a fragment spin $\mathbf{I}$, with the magnetic moment $\boldsymbol{\mu}=g\mu_N\mathbf{I}$, was assumed to follow the classical equation of motion,

$$\frac{d\mathbf{I}}{dt}=\frac{g\mu_N}{h}\,\mathbf{I}\times\mathbf{B}, \tag{5}$$

where $\mathbf{B}=B_0\mathbf{e}_Z+B_1\cos[2\pi\nu(t)t]\mathbf{e}_X$. $\mathbf{e}_Z$ and $\mathbf{e}_X$ denote the unit vectors parallel to the Z and X directions, respectively. Starting from a given direction of $\mathbf{I}$ at $t=0$ and by changing the frequency $\nu(t)$ of the B_1 field linearly in time, the value of $\mathbf{I}$ at $t=T_{\rm rf}$ when the B_1 field was switched off was calculated. Such calculations were performed for $\mathbf{I}(t=0)$ values distributed accordingly to a given polarization P. (In the actual setup, the field strengths B_0 and B_1 had nonuniformities over the stopper area, and also the B_1 strength changed in time because of its frequency dependence. Such details were also included in this simulation.) The resulting average $P'=\langle I_Z\rangle/|\mathbf{I}|$ at $t=T_{\rm rf}$ should represent the polarization after the AFP process, and therefore the ratio $-P'/P$ plotted as a function of the median frequency $\nu=[\nu(0)+\nu(T_{\rm rf})]/2$ should give an expected shape of the $R(\nu)$ spectrum. In fact, the $-P'/P$ curve calculated under the actual conditions in the ^{17}N experiment showed a trapezoidlike shape as represented by the form (4). The value of the width parameter σ in Eq. (4) was determined by comparing the obtained $-P'/P$ curve and Eq. (4).

The fitting yielded $\nu_0=1329.6\pm1.6$ kHz as the peak frequency for ^{17}N, with a rather good accuracy of 0.12%. Below, in the assignment of the error to the experimental magnetic moment, however, the width of the frequency sweep, $\delta\nu/\nu_0=\pm0.60\%$, was quadratically added to the above error of ν_0 from the fitting procedure. Thus the experimental magnetic moment of ^{17}N was deduced as

$$|\mu(^{17}\mathrm{N})|=(0.352\pm0.002)\mu_N, \tag{6}$$

where μ_N denotes the nuclear magneton. No correction was made for the Knight shift and chemical shift since their effects are considered to be much smaller than the experimental error assigned to μ. The Knight shift is estimated as $K\simeq7.8\times10^{-5}$ from the Korringa constant $T_1T=2.7\times10^4$ s K reported for ^{13}C [16], and the chemical shift normally takes the order of 10^{-4}–10^{-5} [12].

For the case of ^{17}B, we first show in Fig. 7(a) the result of a NMR experiment with a broad-bin frequency sweep. In this plot the R value for a sweep over the frequency region 1192–1278 kHz is compared with that obtained without application of the B_1 field (denoted as ''rf off''). This result was obtained after several runs searching for the resonance in a 30% wide frequency region. The R value in Fig. 7(a)

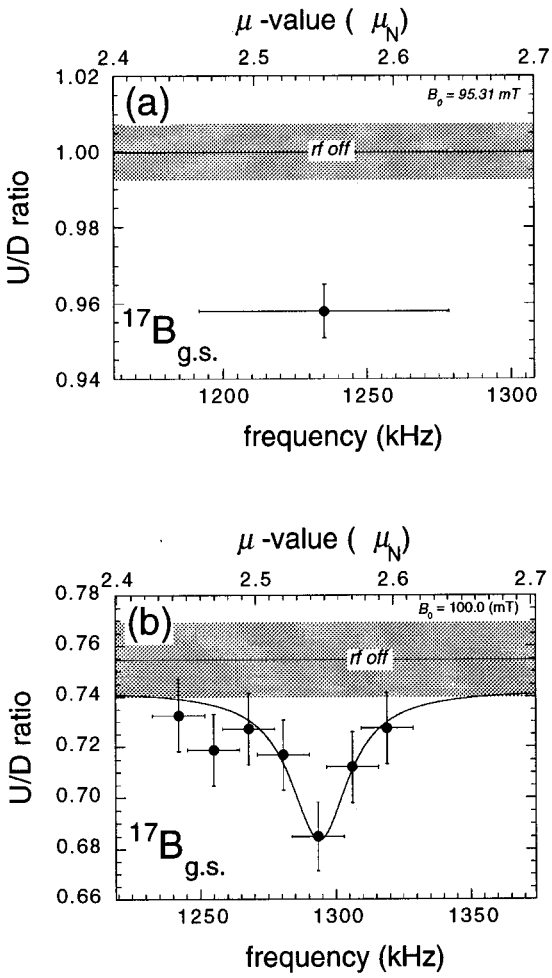

FIG. 7. NMR spectra obtained (a) in a single-bin and (b) in a seven-bin search measurement for the ^{17}B magnetic moment. For the notation, see the caption of Fig. 6. In (a), the R value obtained for the frequency bin $\nu=1192$–1278 kHz showed a clear change from the rf-off value by 4.0 times the standard deviation, indicating that the resonance ν_0 was included in this frequency range. In the succeeding run shown in (b), the above frequency range was devided into seven bins in order to determine a finer value of ν_0.

showed a significant (4.0 times the standard deviation) change and thus indicated that the resonance frequency ν_0 lay in this frequency region.

We then made a seven-bin measurement with a much narrower bin width of $\delta\nu=19.2$ kHz. The NMR spectrum obtained is shown in Fig. 7(b). The experimental magnetic moment of ^{17}B was deduced by least-squares fitting, as done for ^{17}N. In the present case of ^{17}B, however, the functional form of $R(\nu)$ employed for the fitting is quite different from the ^{17}N case: A computer simulation of the AFP process, as described before, was done under the instrumental condition employed for the ^{17}B experiment. The resulting $-P'/P$ curve exhibited a shape which could be well represented by a simple Lorentzian form. This apparent difference in the shape of the spectral function stems from the large difference between the B_1 amplitudes used for the two cases. The shape of the spectrum in the case of ^{17}B was strongly influenced by a broadening effect due to the large B_1 amplitude, while in the ^{17}N case the broadening due to B_1 was much smaller as

compared to the width $\delta\nu$ of the AFP sweep.

Thus, by fitting a Lorentzian function

$$R(\nu)=\frac{C_4}{(\nu-\nu_0)^2+(\Gamma/2)^2}+C_5 \tag{7}$$

with the fixed width parameter $\Gamma=26.4$ kHz, to the experimental spectrum, the experimental magnetic moment of ^{17}B was deduced from the dip frequency $\nu_0=1293.7\pm2.5$ kHz and the width of the frequency sweep, $\delta\nu/\nu_0=\pm0.75\%$, as

$$|\mu(^{17}\mathrm{B})|=(2.545\pm0.020)\mu_N. \tag{8}$$

The Knight shift for B spins in Pt is known [11] to be negligible compared to the error assigned above, and therefore the correction was not made.

IV. DISCUSSION

A. Configurations of the ^{17}N ground state

In an extreme single-particle model, the ground state of ^{17}N is represented by a proton in the $p_{1/2}$ orbit, for which the Schmidt moment is given as $\mu_{\mathrm{Schmidt}}=-0.264\mu_N$. The experimental magnetic moment $\mu_{\mathrm{expt}}=-(0.352\pm0.002)\mu_N$ (hereafter μ_{expt} will be assigned a negative sign taken from the value of μ_{Schmidt}) shows a substantial deviation from μ_{Schmidt}. Most remarkably, the deviation is outwardly directed, while most of the experimental magnetic moments fall into the region between the Schmidt lines [17]. This systematic tendency of magnetic moments is explained by the first-order effect of the $M1$ core polarization [18]. The outward deviation of the presently obtained μ_{expt}, however, is well understood by considering the specific nuclear structure of the ^{17}N ground state, as discussed below.

Considering the ^{16}O as a core, the ^{17}N ground state is predominantly described by one hole in the proton $0p$ shell and two particles in the neutron sd shell. Possible effects, which give rise to the deviation of μ from its single-particle value μ_{Schmidt}, may be investigated in the following two steps.

(i) Let us first assume that the neutrons are coupled to form $J^\pi=0^+$ and examine the polarization effect of the proton core. In this case, since the protons alone have to carry an angular momentum and parity which correspond to the empirical spin and parity $I^\pi=1/2^-$ of $^{17}\mathrm{N}_{\mathrm{g.s.}}$, the proton configuration is uniquely assigned to one with a $p_{1/2}$ hole (unless the $2\hbar\omega$ or higher excitations are considered). Thus no polarization effect of the proton core is expected, and the magnetic moment is just given by the single-particle moment $\mu_{p_{1/2}}$ for the $p_{1/2}$ proton. If we take the bare magnetic operator, $\mu_{p_{1/2}}$ reduces to the Schmidt moment μ_{Schmidt}. In order to make the discussion more quantitative, however, we include the effects [19,20] of the meson exchange currents and second-order configuration mixing by taking the effective g factors [21] of Ref. [19]. Then the single-particle moment is given as

$$\mu_{p_{1/2}}=\langle p_{1/2}|\hat{\mu}|p_{1/2}\rangle \tag{9}$$

$$=\langle p_{1/2}|g_l\hat{l}+g_s\hat{s}+g_p[Y_2(\hat{r})\times\hat{s}]|p_{1/2}\rangle \tag{10}$$

$$=-0.276\mu_N, \tag{11}$$

where the notation of Ref. [19] is followed. For definiteness, we hereafter write the configuration under consideration here as $\psi_0=|(\pi p_{1/2})^{-1}\otimes[(\nu sd)^2]^{J^\pi=0^+}\rangle^{J^\pi=1/2^-}$.

(ii) In the next step the influence of configurations with the sd-shell neutrons coupled to $J^\pi\neq0^+$, which may mix with the dominating configuration ψ_0, is examined. Since the last proton in ψ_0 resides in the $p_{1/2}$ orbit, the $M1$-type configuration mixing is highly suppressed, as pointed out by Noya, Arima, and Horie [18]. This hindrance of the admixture of the $J^\pi=1^+$ neutron configuration, along with the absence of the proton core polarization as described in (i), is considered as the reason why the inward deviation of μ from μ_{Schmidt} does not occur. Then, the most likely configurations which can admix to ψ_0 and alter the magnetic moment are those with the sd neutrons coupled to form $J^\pi=2^+$, such as $\psi_A=|(\pi p_{3/2})^{-1}\otimes[(\nu d_{5/2})^2]^{J^\pi=2^+}\rangle^{J^\pi=1/2^-}$ and $\psi_B=|(\pi p_{3/2})^{-1}\otimes[(\nu s_{1/2})(\nu d_{5/2})]^{J^\pi=2^+}\rangle^{J^\pi=1/2^-}$. This presumption indeed holds true in the shell-model calculations presented in the next subsection.

Thus the ^{17}N ground state may be modeled in the following wave function:

$$\psi=c_0\psi_0+c_A\psi_A+c_B\psi_B. \tag{12}$$

Here the contribution of the neutron $d_{3/2}$ orbit is neglected for the sake of simplicity. The magnetic moment μ is then expressed as

$$\begin{aligned}\mu(^{17}\mathrm{N})&=\langle\psi|\hat{\mu}|\psi\rangle\\&=c_0^2\langle\psi_0|\hat{\mu}|\psi_0\rangle+c_A^2\langle\psi_A|\hat{\mu}|\psi_A\rangle+c_B^2\langle\psi_B|\hat{\mu}|\psi_B\rangle\end{aligned} \tag{13}$$

in terms of the diagonal matrix elements of the magnetic moment operator $\hat{\mu}$,

$$\langle\psi_0|\hat{\mu}|\psi_0\rangle=\mu_{p_{1/2}}, \tag{14}$$

$$\langle\psi_A|\hat{\mu}|\psi_A\rangle=-\tfrac{1}{3}\mu_{p_{3/2}}+\tfrac{2}{5}\mu_{d_{5/2}}=-2.01, \tag{15}$$

and

$$\langle\psi_B|\hat{\mu}|\psi_B\rangle=-\tfrac{1}{3}\mu_{p_{3/2}}-\tfrac{1}{3}\mu_{s_{1/2}}+\tfrac{7}{15}\mu_{d_{5/2}}=-1.54. \tag{16}$$

In Eq. (13), the off-diagonal term between ψ_A and ψ_B, which arises from the g_p term of the effective operator $\hat{\mu}$, has been neglected because of its small size.

We can easily understand from Eqs. (15) and (16) that the mixing of the neutron 2^+ configuration causes the magnetic moment to shift outward from the Schmidt line, because two matrix elements $\langle\psi_A|\hat{\mu}|\psi_A\rangle$ and $\langle\psi_B|\hat{\mu}|\psi_B\rangle$ have negative sign. We also note that these matrix elements are distinctively larger than that for the major configuration $\langle\psi_0|\hat{\mu}|\psi_0\rangle$. This implies that even small probabilities $|c_A|^2$ and $|c_B|^2$ may substantially influence the value of the magnetic moment. By setting $\langle\psi|\hat{\mu}|\psi\rangle=\mu_{\mathrm{expt}}$ we obtain $|c_A|^2+0.73|c_B|^2=4.4\%$. Thus, to accommodate the $\langle\psi|\hat{\mu}|\psi\rangle$ to the experimental μ value, a total (4.4–6.0)% admixture of the configurations with sd neutrons coupled to 2^+ is required.

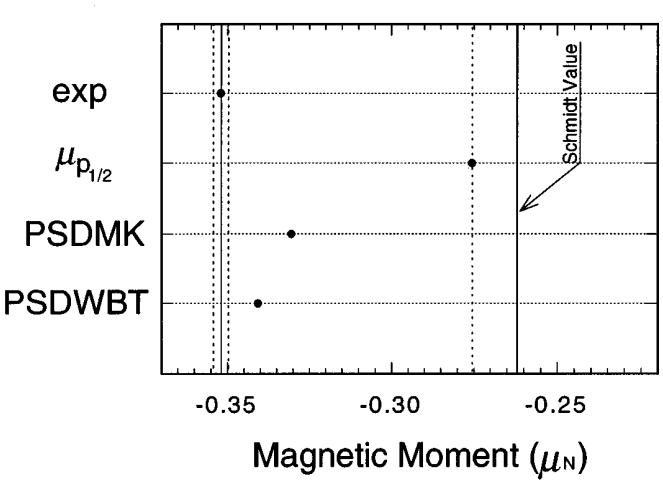

FIG. 8. Comparison of the experimental μ value (exp) for ^{17}N with the theoretical predictions. For the symbols denoting the theories, see text.

B. Comparison with shell model calculations

In Fig. 8 the experimental $\mu(^{17}\mathrm{N})$ value is compared with the results of shell-model calculations. Two different sets of effective interactions were used. The first one, referred to as PSDMK in Ref. [14], consists of the Cohen-Kurath interaction [22] as the p-shell part, the Preedom-Wildenthal interaction [23] as the sd-shell part, and the Millener-Kurath interaction [24] as the p-sd cross-shell part. The second one, referred to as PSDWBT, consists of the Warburton-Brown interaction [25] as the p-shell and p-sd cross-shell parts and the USD interaction [26] as the sd-shell part. As shown in Table I, for both interactions the configurations ψ_0, ψ_A, and ψ_B account for more than 99% of the ^{17}N ground state, indicating that the modeling in Sec. IV A is well justified. In the following, we define the deviation $\delta\mu$ of the ^{17}N magnetic moment $\mu(^{17}\mathrm{N})$ from the single-particle moment $\mu_{p_{1/2}}$ as $\delta\mu \equiv \mu(^{17}\mathrm{N}) - \mu_{p_{1/2}}$. The calculations with the PSDMK and PSDWBT interactions predict the deviation as $\delta\mu = -0.055\mu_N$ and $-0.065\mu_N$, respectively, in fairly good agreement with the observation $\delta\mu = -0.076\mu_N$. In terms of the amount of the neutron 2^+ admixture, the PSDWBT (PSDMK) calculation yields a total 2.8% (4.6%) probability to be compared to the empirically obtained range (4.4–6.0)% in the previous subsection.

TABLE I. Wave function for the ground state of ^{17}N calculated with the PSDWBT and PSDMK interactions. The coefficients c_i ($i=0$, A, and B) are defined in Eq. (12) in the text.

		Probability $\lvert c_i\rvert^2$	
Symbol	Configuration	PSDWBT	PSDMK
ψ_0	$(\pi p_{1/2})^{-1}\otimes[(\nu d_{5/2})^2]^{0^+}$	63.4%	62.8%
	$(\pi p_{1/2})^{-1}\otimes[(\nu s_{1/2})^2]^{0^+}$	26.9%	25.1%
ψ_A	$(\pi p_{1/2})^{-1}\otimes[(\nu d_{3/2})^2]^{0^+}$	6.5%	6.7%
	$(\pi p_{3/2})^{-1}\otimes[(\nu d_{5/2})^2]^{2^+}$	2.2%	3.8%
ψ_B	$(\pi p_{3/2})^{-1}\otimes[(\nu s_{1/2})(\nu d_{5/2})]^{2^+}$	0.6%	0.8%
Sum		99.5%	99.3%

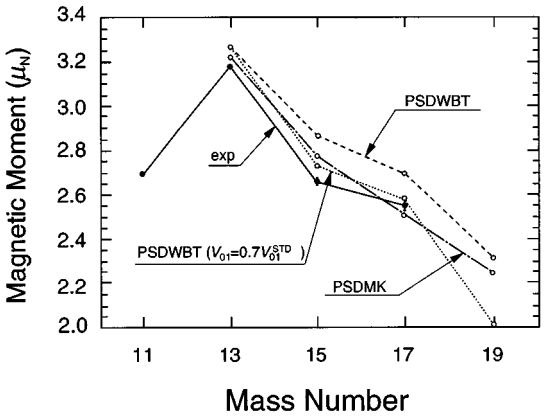

FIG. 9. Experimental and theoretical values of μ for the odd-mass B isotopes. Exp, the experimental values; PSDWBT, the shell-model calculations [14] with the PSDWBT [14,25] interaction; PSDWBT ($0.7V_{01}^{\mathrm{std}}$), the PSDWBT calculations with $|V_{01}|$ values reduced by 30% [i.e., the three matrix elements $\langle(d_{5/2})^2|V|(d_{5/2})^2\rangle^{J^\pi=0^+}$, $\langle(s_{1/2})^2|V|(s_{1/2})^2\rangle^{J^\pi=0^+}$, and $\langle(d_{3/2})^2|V|(d_{3/2})^2\rangle^{J^\pi=0^+}$ are multiplied by a common factor 0.7]; PSDMK, the shell-model calculations with the PSDMK [24] interaction.

In the above calculated values for $\delta\mu$ as well as for the 2^+ component, a slight tendency to be smaller than the experiment might be noticed. This point will be investigated later in the next section in conjunction with the ^{17}B result.

C. Magnetic moment of ^{17}B

The experimental magnetic moment μ_{expt} for ^{17}B is plotted in Fig. 9, together with those for the other odd-mass B isotopes. The μ_{expt} value, as a function of the mass number A, takes a maximum at $A=13$, where the neutron sd orbits are vacant, and shows a steep decrease for larger A. The $p_{3/2}$ proton single-particle value is calculated as $\mu_{p_{3/2}} = +3.80\mu_N$. The μ_{expt} values are substantially smaller than $\mu_{p_{3/2}}$. The quenching of μ at $A=13$ is well accounted for by the first-order effect of the $M1$ core polarization [19]. The magnitude of this effect is found to be almost independent of A, and therefore the extra quenching observed for $A>13$ should be explained by other mechanisms.

The results of shell-model calculations with the PSDWBT interaction are shown in Fig. 9 by open circles connected with thin lines. For $A=13$, the calculated μ reproduces the observed moment well, and the quenching of $\mu(^{13}\mathrm{B})$ is found to stem from the $M1$ core polarization in terms of the off-diagonal matrix elements between the $[(\pi p_{3/2})^3]^{J^\pi=3/2^-}$ and $[(\pi p_{3/2})^2\otimes(\pi p_{1/2})]^{J^\pi=3/2^-}$ configurations. For $A>13$, the calculated μ decreases, and the inspection of the resulting wave function reveals that this extra quenching of μ for $A>13$ is produced by the admixing of configurations with the sd neutrons coupled to $J^\pi=2^+$, just as the excess μ is produced in the ^{17}N nucleus. The observed quenching, however, is larger than the calculations, suggesting that the contribution of the component with $J^\pi=2^+$ sd-shell neutrons is underestimated in the PSDWBT calculation.

Figure 9 also includes μ values calculated with the PSDMK interaction. For ^{17}B, the calculated μ appears in rather good agreement with the experiment. However, the mass-

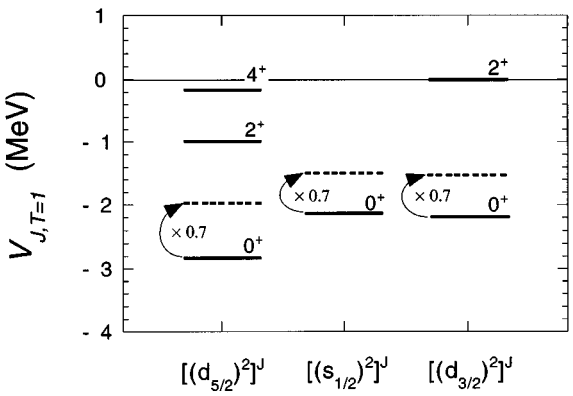

FIG. 10. Diagonal two-body matrix elements (V_{JT}) of the PSDWBT interaction for the neutron $[(d_{5/2})^2]^J$, $[(s_{1/2})^2]^J$, and $[(d_{3/2})^2]^J$ configurations. The thick dashed bars indicate the effect of the 30% reduction of $|V_{01}|$ from the standard value.

number dependence of μ is not reproduced well by the PSDMK calculation. We also note that calculations with this interaction failed to reproduce low-lying energy levels of ^{16}N and ^{17}N [27]. In view of these facts, we consider that this agreement of $\mu(^{17}\mathrm{B})$ is not satisfactory and further investigate the comparison of the experiment with the PSDWBT calculations in the next section.

V. IMPLICATION OF THE RESULTS

A. Analysis in terms of reduced pairing energy: The ^{17}B case

As shown in the preceding section, the experimental magnetic moment of ^{17}B suggests that the contribution of the $J^\pi=2^+$ neutron configuration is larger than the shell-model calculation with the PSDWBT interaction. In this section we investigate for a while a physical implication drawn from such a phenomenon. The tendency for a neutron pair to couple to $J^\pi=2^+$ rather than $J^\pi=0^+$ should be largely governed by the difference between the two-body matrix elements $V_{J=2,T=1}$ and $V_{J=0,T=1}$ of the shell-model interactions. Here $V_{J,T}$ denotes a diagonal matrix element of a two-body effective interaction in a channel with angular momentum J and isospin T, for particles within the sd orbits. Thus, in shell models, the contribution of the 2^+ coupling increases when either the pairing energy $|V_{01}|$ is reduced or the energy $|V_{21}|$ is increased. From this point of view, it is interesting to note that a signature for the diminished pairing energy is given by recent study of binding energies for the neutron-rich C isotopes [28]. They show that calculations with the WBP interaction [25] systematically predict overbinding for the even C isotopes ^{16}C, ^{18}C, and ^{20}C.

The PSDWBT calculation was performed with reduced $|V_{01}|$ values for the sd neutrons. As indicated by a dotted line in Fig. 9, the agreement is gained for the ^{17}B magnetic moment when $|V_{01}|$ is reduced by 30%. The mass-number dependence of μ from $A=13$ to 17 is also reproduced quite well. As going to $A=19$, the predicted μ rapidly decreases. It would be interesting to measure the ^{19}B magnetic moment, but the measurement would require substantial improvement in the ^{19}B yield. In Fig. 10 the V_{JT} values for the neutron $(d_{5/2})^2$, $(s_{1/2})^2$, and $(d_{3/2})^2$ configurations are plotted. The 30% reduction in $|V_{01}|$ of the PSDWBT interaction is indicated by the dashed line.

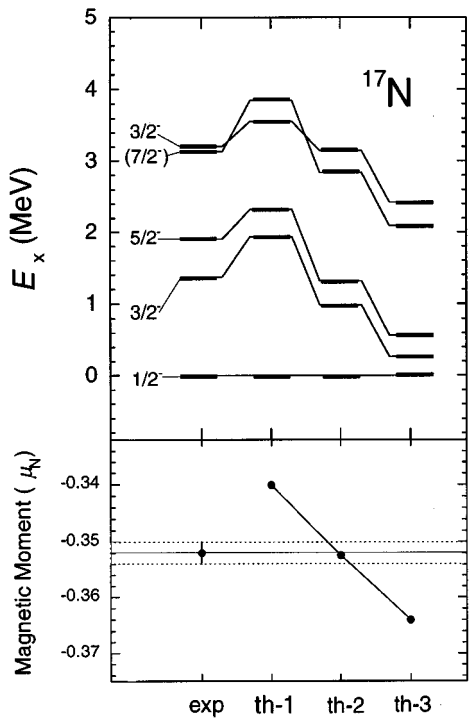

FIG. 11. V_{01} dependence of the calculated magnetic moment (lower) and normal-parity levels (upper) of ^{17}N. The calculations are made with the PSDWBT interaction and with $V_{01}=V_{01}^{\mathrm{std}}$ (th-1), $V_{01}=0.7V_{01}^{\mathrm{std}}$ (th-2), or $V_{01}=0.3V_{01}^{\mathrm{std}}$ (th-3), where V_{01}^{std} stands for the standard value of V_{01} taken in [14]. The experimental ones (exp) are also shown.

B. Cases of ^{17}N and other isotones

As seen in Sec. IV B, the ^{17}N magnetic moment is accounted for within $(0.01-0.02)\mu_N$ accuracies by the PSDMK and PSDWBT models even without altering the $|V_{01}|$ value. We note, however, that the predicted $\delta\mu$ values show in common a tendency to be smaller in magnitude than the experiment. This implies that the contribution of the $J^\pi=2^+$ neutron configurations may be slightly underpredicted, since $\delta\mu$ for ^{17}N mainly stems from the ψ_A and ψ_B components as shown in Sec. IV A. It is therefore worthwhile to examine the above hypothesis of the reduced pairing energy also in the case of ^{17}N and other nuclei.

In Fig. 11, the theoretical μ and the low-lying energy levels of ^{17}N are plotted for several $|V_{01}|$ values. As evident in the figure, a 30% reduction of $|V_{01}|$ leads to a remarkably good agreement with the experiment concerning the magnetic moment. Moreover, the energy levels become better reproduced by the calculation.

We next investigate the pairing energy in terms of observables other than the magnetic moment. The binding energy difference between ^{17}N and ^{15}N is calculated as 9.16 MeV with the PSDWBT interaction, while it is found to be 8.37 MeV experimentally. A 30% reduction of the pairing energy leads to a calculated values of 8.15 MeV, showing much better agreement with the experiment. This may indicate that

TABLE II. Comparison of the experimental and calculated magnetic moments (in unit of μ_N) for the $N=10$, odd-Z isotones. The calculations are made with the PSDWBT interaction by using (a) the standard values of $|V_{01}|$ and $|V_{21}|$, (b) 70% of the standard value for $|V_{01}|$, and (c) $|V_{21}|$ augmented by 1 MeV from the standard value.

		(a)		(b)		(c)	
Nucleus	$\mu_{\rm expt}$	$\mu_{\rm calc}$	$\delta\mu/\mu_{\rm expt}$	$\mu_{\rm calc}$	$\delta\mu/\mu_{\rm expt}$	$\mu_{\rm calc}$	$\delta\mu/\mu_{\rm expt}$
^{15}B	(+)2.650 (13)	2.865	8.1%	2.727	2.9%	2.832	6.9%
^{17}N	(−)0.352 (2)	−0.341	−3.2%	−0.352	0.1%	−0.352	0.0%
^{19}F	2.628868(8)	2.706	2.9%	2.723	3.6%	2.722	3.5%

the pairing energy $|V_{01}|$ in ^{17}N is smaller than assumed in the standard shell model.

The hypothesis of the reduced $|V_{01}|$ in neutron-rich nuclei is further examined for the $N=10$ isotones ^{15}B, ^{16}C, ^{18}O, and ^{19}F in Table II and Fig. 12. These nuclei have two neutrons in the sd orbits in common with the ^{17}N nucleus. The p shell for protons, however, is open for the first two nuclei, while it is closed for the others. The experimental and calculated magnetic moments for the odd-Z, $N=10$ isotones are compared in Table II. The calculations were made with the PSDWBT interaction and by changing the $|V_{01}|$ or $|V_{21}|$ values. The agreement of the calculation with the experiment for the ^{15}B magnetic moment is drastically improved by the 30% reduction of $|V_{01}|$. In contrast, the same reduction worsens the agreement in the magnetic moment of ^{19}F, which has the closed proton p shell. A similar trend is observed in the energy levels in ^{16}C and ^{18}O, as shown in Fig. 12. The 30% reduction of $|V_{01}|$ improves the agreement in the ^{16}C levels, whereas the calculated excitation energies become too low in the case of the p-shell closed isotone ^{18}O. All these observations are consistent with an assumption that the reduction by about 30% in the $J^\pi=0^+$ coupling energy for the sd-shell neutrons takes place in neutron-rich nuclei whose proton p shell is open.

VI. CONCLUSION

The capability of the intermediate-energy projectile fragmentation reaction to produce spin-polarized unstable nuclei has enabled to extend the measurement of magnetic moments to the neutron-rich nuclei ^{17}N and ^{17}B.

The experimental magnetic moment obtained for ^{17}N is found to be considerably enhanced in magnitude from its single-particle value. An analysis of the enhancement, based on the simplifying feature intrinsic to a nucleus with a $p_{1/2}$ valence nucleon, provides reliable information on the ground state wave function. Shell-model calculations give a fairly good account of the observed magnetic moment, though the experimental $\mu(^{17}\mathrm{N})$ may be slightly larger than the calculations.

For ^{17}B, the observed magnetic moment was found to be overquenched as compared to the standard shell-model calculation. The overquenching in $\mu(^{17}\mathrm{B})$ is ascribed to an enhanced contribution of the $J^\pi=2^+$ neutron configurations. This result is accounted for by assuming that the pairing energy for the sd neutrons to form $J^\pi=0^+$ is considerably reduced. This phenomenon of the reduction in the sd-neutron pairing energy may be considered as manifestation of the weakening of the coupling between excess neutrons and a core, in nuclei far from stability. For example, the theoretical V_{01} value for two $d_{5/2}$ neutrons in Ref. [29] includes correction of −1.06 MeV from the renormalization of the two-body interaction due to the polarization of the core. The experimentally inferred V_{01} reduction of 30%, amounting to a 0.82-MeV reduction of $|V_{01}|$ for the $(d_{5/2})^2$ configuration, implies an 80% quenching of the renormalization correction. It is interesting to note here that also the neutron effective charge was indicated to diminish by 80% in the measured quadrupole moments of ^{15}B [3].

The above idea of a weakened coupling between excess neutrons and the core naturally implies that the reduction in the pairing energy is a phenomenon characteristic of weakly bound nuclei. We must, however, draw attention to the pos-

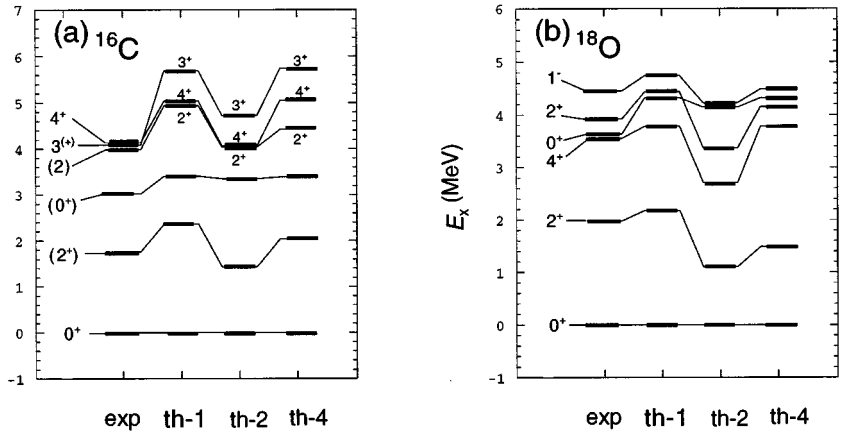

FIG. 12. Dependence of the calculated low-lying energy levels for ^{16}C and ^{18}O on V_{01} and V_{21}. The calculations are made with the PSDWBT interaction, and with the standard values for V_{01} and V_{21} (th-1), with V_{01} reduced by 30% from the standard value (th-2) or with V_{21} lowered by 1.0 MeV from the standard value (th-4). In the last case, only the matrix element $\langle(d_{5/2})^2|V|(d_{5/2})^2\rangle^{J^\pi=2^+}$ was lowered. The experimental data are also shown (exp).

sibility of another scenario. The reduction of $|V_{01}|$ also improved agreement in the magnetic moment and low-lying levels of ^{17}N. Similar improvements were obtained for other $N=10$ isotones whose proton p shell is open, while the agreement was worsened for those with a closed p shell. These observations might suggest that the presence of a proton hole in the p shell is essential for the reduction of the sd-neutron pairing energy. This point remains a subject of further investigation.

ACKNOWLEDGMENTS

The authors are grateful to the staffs of the RIKEN Ring Cyclotron for their support during the running of the experiments. The authors are also indebted to H. Kumagai for developing the PSG module. They would like to express special thanks to Prof. T. Otsuka for illuminating discussions and valuable comments. The shell-model calculations were carried out by using the program OXBASH coded by B. A. Brown *et al.* Two of the authors, H. O. and N. F., acknowledge support from the Special Researchers' Basic Program of Science and Technology Agency of Japan. H.U. and H.S. are grateful to the Japan Society for the Promotion of Science for Young Scientists for support. This work was partly supported by a Grant-in-Aid in Scientific Research of the Japanese Ministry of Education, Science and Culture.

[1] B. M. Sherrill, in *Proceedings of the Second International Conference on Radioactive Nuclear Beams*, 1991, edited by Th. Delbar (Hilger, Bristol, 1992), p. 3.
[2] H. Okuno, K. Asahi, H. Ueno, H. Izumi, H. Sato, M. Adachi, T. Nakamura, T. Kubo, N. Inabe, A. Yoshida, N. Fukunishi, T. Shimoda, H. Miyatake, N. Takahashi, W.-D. Schmidt-Ott, and M. Ishihara, Phys. Lett. B **354**, 41 (1995).
[3] H. Izumi, K. Asahi, H. Ueno, H. Okuno, H. Sato, K. Nagata, Y. Hori, M. Adachi, N. Aoi, A. Yoshida, G. Liu, N. Fukunishi, and M. Ishihara, Phys. Lett. B **366**, 51 (1996).
[4] D. R. Tilley, H. R. Weller, and C. M. Cheves, Nucl. Phys. **A564**, 1 (1993).
[5] G. Audi and A. H. Wapstra, Nucl. Phys. **A565**, 1 (1993).
[6] E. Litard, J. F. Braundet, F. Glasser, S. Kox, Tsan Ung Chan, G. J. Costa, C. Heitz, Y. El Masri, F. Hanappe, R. Bimbot, D. Guillemaud-Mueller, and A. C. Mueller, Europhys. Lett. **13**, 401 (1990).
[7] K. Asahi, M. Ishihara, N. Inabe, T. Ichihara, T. Kubo, M. Adachi, H. Takahashi, M. Kouguchi, M. Fukuda, D. Mikolas, D. J. Morrissey, D. Beaumel, T. Shimoda, H. Miyatake, and N. Takahashi, Phys. Lett. B **251**, 488 (1990).
[8] H. Okuno, K. Asahi, H. Sato, H. Ueno, J. Kura, M. Adachi, T. Nakamura, T. Kubo, N. Inabe, A. Yoshida, T. Ichihara, Y. Kobayashi, Y. Ohkubo, M. Iwamoto, F. Ambe, T. Shimoda, H. Miyatake, N. Takahashi, J. Nakamura, D. Beaumel, D. J. Morrissey, W.-D. Schmidt-Ott, and M. Ishihara, Phys. Lett. B **335**, 29 (1994).
[9] T. Kubo, M. Ishihara, N. Inabe, H. Kumagai, I. Tanihata, K. Yoshida, T. Nakamura, H. Okuno, S. Shimoura, and K. Asahi, Nucl. Instrum. Methods Phys. Res. B **70**, 309 (1992).
[10] J. A. Winger, B. M. Sherrill, and D. J. Morrissey, Nucl. Instrum. Methods Phys. Res. B **70**, 41 (1992).
[11] R. Williams, L. Pfeiffer, J. Wells, and L. Madansky, Phys. Rev. C **2**, 1219 (1970).
[12] A. Abragam, *The Principle of Nuclear Magnetism* (Clarendon, Oxford, 1961).
[13] F. Ajzenberg-Selove, Nucl. Phys. **A460**, 1 (1986).
[14] B. A. Brown, A. Etchegoyen, and W. D. M. Rae, Computer code OXBASH, MSU Cyclotron Laboratory Report No. 524, 1986.
[15] J.-P. Dufour, R. Del Moral, F. Hubert, D. Jean, M. S. Pravikoff, A. Fleury, A. C. Mueller, K.-H. Schmidt, K. Sümmerer, R. Hanelt, J. Frehaut, M. Beau, and G. Giraudet, Phys. Lett. B **206**, 195 (1988).
[16] G. P. Carver, Phys. Rev. B **2**, 2284 (1970).
[17] H. Morinaga and T. Yamazaki, *In-Beam Gamma-Ray Spectroscopy* (North-Holland, Amsterdam, 1976).
[18] H. Noya, A. Arima, and H. Horie, Suppl. Prog. Theor. Phys. **8**, 33 (1958).
[19] A. Arima, K. Shimizu, W. Bentz, and H. Hyuga, Adv. Nucl. Phys. **18**, 1 (1987).
[20] I. S. Towner, Phys. Rep. **155**, 263 (1987).
[21] Specifically, we take following g values: $g_l=1.104$, $g_s=5.309$, and $g_p=0.951$ for p-shell protons, $g_l=-0.016$, $g_s=-3.571$, and $g_p=-0.965$ for sd-shell neutrons. We take these g values in all the calculations presented hereafter.
[22] S. Cohen and D. Kurath, Nucl. Phys. **73**, 1 (1965).
[23] B. M. Preedom and B. H. Wildenthal, Phys. Rev. C **6**, 1633 (1972).
[24] D. J. Millener and D. Kurath, Nucl. Phys. **A255**, 315 (1975).
[25] E. K. Warburton and B. A. Brown, Phys. Rev. C **46**, 923 (1992).
[26] B. H. Wildenthal, Prog. Part. Nucl. Phys. **11**, 5 (1984).
[27] F. C. Barker, Aust. J. Phys. **37**, 17 (1984).
[28] D. Bazin, B. A. Brown, J. Brown, M. Fauerbach, M. Hellström, S. E. Hirzebruch, J. H. Kelley, R. A. Kryger, D. J. Morrissey, R. Pfaff, C. F. Powell, B. M. Sherrill, and M. Thoennessen, Phys. Rev. Lett. **74**, 3569 (1995).
[29] T. T. S. Kuo and G. E. Brown, Nucl. Phys. **85**, 40 (1966).